

Nanoscale ferromagnetic chromium oxide film from gas-phase nanocluster deposition

Yanping Chen, Kui Ding, Ling Yang, Bo Xie, Fengqi Song, Jianguo Wan, Guanghou Wang, and Min Han^{a)}

National Laboratory of Solid State Microstructures and Department of Materials Science and Engineering, Nanjing University, Nanjing 210093, People's Republic of China

(Received 21 January 2008; accepted 12 April 2008; published online 1 May 2008)

Ferromagnetic film of densely packing chromium oxide nanoparticles has been fabricated by vacuum deposition of chromium oxide clusters at room temperature. The clusters were generated with a magnetron plasma gas aggregation source by introducing a mixture of argon and oxygen as buffer gas. A magnetic hysteresis loop similar to that of bulk CrO₂ was observed in a wide temperature range. The rise in the ferromagnetic property of the film was attributed to the nanoscale CrO₂ composition. The work demonstrates a simple way to fabricate ferromagnetic films of chromium oxide nanoparticles under high-vacuum compatible low temperature condition. © 2008 American Institute of Physics. [DOI: 10.1063/1.2919077]

Chromium dioxide is recently of considerable interest due to its attractive potential for use in spintronic heterostructures. It is a unique ferromagnetic oxide that is predicted to be a half-metallic ferromagnet at room temperature and has a half-metallic band structure fully spin polarized at the Fermi level,¹⁻³ which makes CrO₂ a good candidate for use as magnetic components in magnetoelectronic devices that require a large spin polarization, such as magnetic tunnel junctions and spin valves.

However, CrO₂ is not a stable Cr–O phase under normal conditions, and the magnetic properties of chromium oxides are highly sensitive to changes in stoichiometric composition. At atmospheric pressure, CrO₂ is easy to decompose into insulating antiferromagnetic Cr₂O₃ phase when heated. Such metastable nature generates difficulties on fabricating CrO₂ materials and special methods are needed. High-pressure, thermal decomposition method has been used in industry, which produces microscale needle powders. Chemical vapor deposition (CVD) technique was discovered in the late 1970s, and perhaps is still the most effective way for epitaxial CrO₂ film fabrication.^{4,5} Nevertheless, it is believed ineffectual to obtain CrO₂ films with standard high-vacuum physical deposition methods, such as molecular beam epitaxy or sputtering.⁶ Challenge still remains on developing an efficient way for fabricating CrO₂ films at sufficiently low temperatures,⁷ which is important for many device applications.

Gas-phase nanocluster synthesis and deposition provides a well-developed process able to produce novel nanoscale materials with a high level of control on physicochemical properties such as phase and composition.⁸ Previous study⁹ showed the possibility to generate two different classes of very stable and chemically inert Cr_nO_m clusters by controlling the formation condition of a laser ablation cluster source combined with a fast-flow tube reaction apparatus. When substoichiometric clusters were first formed and then oxidized, Cr_nO_{2n+2} series were obtained. Whereas the clusters produced under energetic conditions favored Cr_nO_{3n} series.

Especially, Cr_nO_{2n+2} clusters were ferromagnetic as predicted from *ab initio* calculations. In this letter, we report that ferromagnetic chromium oxide film could be fabricated by depositing chromium oxide clusters generated with a magnetron plasma gas aggregation cluster source. The deposition process is under low temperature condition and high-vacuum compatible. The film has a magnetic hysteresis loop similar to that of bulk CrO₂. Furthermore, it has a densely packing nanoparticle-based structure, which may promise as interesting nanomagnetism model system with potential applications.

The gas-phase clusters to be deposited were generated in a magnetron plasma gas aggregation cluster source described elsewhere in detail.¹⁰ The magnetron discharge was operated in a liquid nitrogen cooled aggregation tube. A stream of pure (99.99%) argon gas was introduced through a ring structure close to the surface of a chromium target with 99.9% purity to maintain the discharge. Another stream of argon mixed with a small fraction of pure oxygen was fed as a buffer gas through a gas inlet near the magnetron discharge head. A constant total pressure of 200 Pa and a 2% oxygen-argon ratio was maintained. Clusters were formed from the atoms sputtered from the target. During this process, charged particles in the discharge-generated plasma acquired high kinetic energies and collided with the neutrals in the gas, causing the formation of very reactive species. Therefore the clusters were efficiently oxidized. To avoid strong arcing that was often accompanied with dc reactive sputtering, a dc pulse power was used with a 30 kHz pulsing frequency at 0.8 duty cycle. The clusters were swept by the gas stream out of the aggregation tube into vacuum through a nozzle. Then they continued to pass through a skimmer into a high-vacuum (10⁻⁷ Torr) chamber and deposited on the substrate. A deposition rate of 1 Å/s, monitored by a quartz crystal microbalance, was obtained with a discharge power of 90 W.

The transmission electron microscope (TEM) image of a typical low coverage deposit sampled on an amorphous carbon film of TEM grid is shown in Fig. 1(a). Individual nanoparticles with size ranging from several nanometers to about 20 nm can be clearly distinguished, although some of them are coagulated as a result of irreversibly sticking without

^{a)} Author to whom correspondence should be addressed. Electronic mail: sjhanmin@nju.edu.cn.

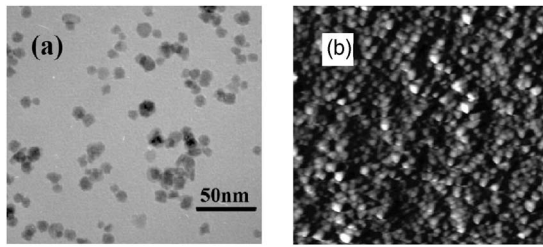


FIG. 1. (a) TEM image of a typical low coverage deposit sampled on an amorphous carbon film of TEM grid with short deposition time. (b) $1600 \times 1600 \text{ nm}^2$ AFM image of a heavily deposited film sampled on a flat silica glass sheet.

coalescence. The nanoparticles are nearly spherical. The diameters of the smallest ones are around 2 nm, which may represent the size of the original clusters from the gas phase. Selected area electron diffraction gives no distinguishable diffraction rings on the pattern, indicating that the nanoparticles are amorphous, or to say, the bulklike crystalline structures have not been developed in these particles. Figure 1(b) gives an atomic force microscope (AFM) image of a heavily deposited film sampled on a flat silica glass sheet. It can be observed that the nanoparticles are densely packed, forming a uniformly continuous film, but each individual nanoparticle is still clearly distinguishable.

To analyze the oxidation state of the sample, x-ray photoelectron spectroscopy (XPS) was carried out with a ESCALABMK-II spectrometer using a monochromatic Mg $K\alpha$ source. Figure 2 shows the photoemission data of the Cr $2p$ core levels measured from a film of chromium oxide nanoparticles. The binding energy of Cr $2p_{3/2}$ core level for the sample is about 576.5 eV, which is well shifted from the 574.1 eV line of metallic chromium measured from a reference chromium nanoparticle sample deposited at same condition without introducing of oxygen. The photoemission data of Fig. 2 were not changed after the sample surface was cleaned with Ar ion sputtering, indicating that the nanoparticles were completely oxygen passivated. Nevertheless, the peak of the Cr $2p_{3/2}$ core level in Fig. 2 is situated between the accepted binding energies for Cr_2O_3 and CrO_2 (576.8 versus 576.3 eV).¹² The difference between the binding energies of these two oxidation states is so small that it is

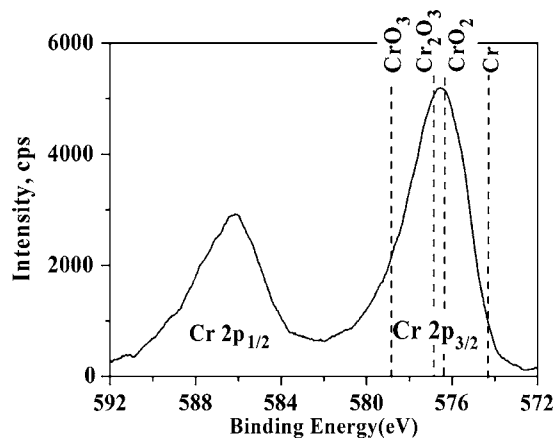


FIG. 2. XPS Cr $2p$ core level spectrum of the chromium oxide nanoparticle assembled film. Vertical dash lines indicate binding energies of chromium oxides CrO_3 (578.8 eV),¹¹ CrO_2 (576.3 eV),¹² Cr_2O_3 (576.8 eV),¹² and metallic chromium (574.3 eV).¹¹

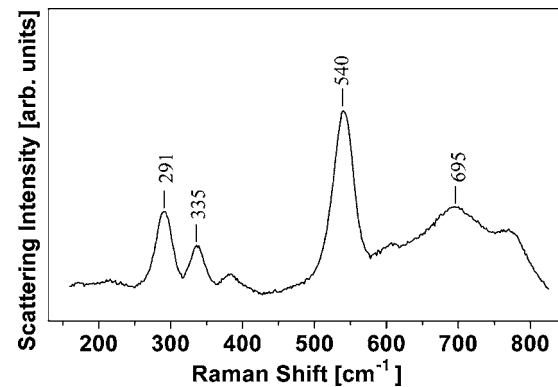


FIG. 3. Raman spectrum of the chromium oxide nanoparticle assembled film.

insufficient to distinguish the Cr_2O_3 and CrO_2 components of the sample merely from XPS measurement.

The chromium oxide phases were further characterized by micro-Raman spectroscopy (NT-MDT NTEGRA Spectra) with 473 nm laser excitation. As shown in Fig. 3, the Raman spectrum reveals an intense peak assigned to the B_{2g} mode of CrO_2 (Ref. 13) at 695 cm^{-1} Raman shift. The peak is broad due to the high level of amorphization of the chromium oxide nanoparticles. In addition, the peaks at about 291, 335 and 540 cm^{-1} can be assigned to the Raman modes of Cr_2O_3 , which are redshifted by about 15 cm^{-1} compared with the bulk Cr_2O_3 crystal. Such redshifts have been reported for pure amorphous Cr_2O_3 powder with 10 nm grain size.¹⁴ Although the most intense A_{1g} band of Cr_2O_3 at 540 cm^{-1} has an intensity comparable to the B_{2g} band of CrO_2 , the relative content of CrO_2 is not able to be estimated from the intensity ratio between CrO_2 B_{2g} and Cr_2O_3 A_{1g} band, since surface reactions such as $2\text{CrO}_2 \rightarrow \text{Cr}_2\text{O}_3 + 1/2\text{O}_2$ may occur and change the final composition at the surface of the specimen, while Raman spectroscopy is surface sensitive. However, it is clear that the Cr_2O_3 content is not the dominant of the specimen.

Magnetic measurements were performed using a superconducting quantum interference device (Quantum Design MPMS XL-7) at various temperatures after a film with an equivalent deposition thickness of 1000 Å had been cooled from room temperature in a field of 10 kOe. Figure 4 shows a typical magnetic hysteresis loop taken at 5 K. The sample exhibits a gradual and rounded hysteresis loop which is ex-

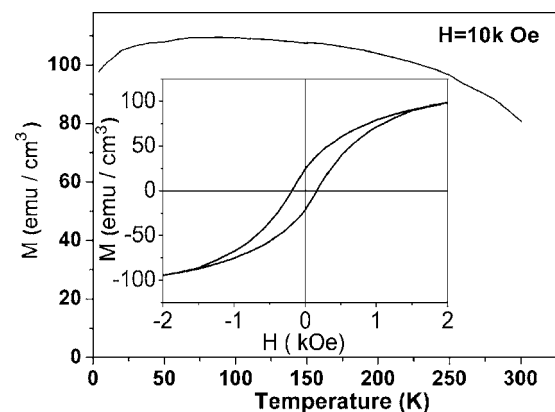


FIG. 4. Temperature-dependent magnetization curve of chromium oxide nanoparticle film measured at 10 kOe. (Inset) magnetic hysteresis loop taken at 5 K.

pected for the average of the random orientation of spherical nanoparticles and has a fractional remanence (ratio of remanence to saturation magnetization) of about 0.25, similar to that for the polycrystalline bulk CrO₂ film.^{3,15} At 5 K, the coercive field (H_c) is determined to be 168 Oe, well below that measured from commercial needle-shaped CrO₂ powders (800–1000 Oe) (Ref. 16) but significantly larger than that measured for polycrystalline CrO₂ film (40 Oe).³ The commercial CrO₂ powder has an aspect ratio of 7:1 or more, the large shape anisotropy induces high coercivity.¹⁷ In our sample, the nanoparticles are near spherical so that the contribution from anisotropy enhancement is small. It seems the chromium oxide nanoparticles have large coercive fields, which may originate from the single domain behavior of the nanoparticles with such small sizes.¹⁸

The saturation magnetization (M_s) observed from the hysteresis loop is about 98 emu/cm³ at 5 K. If a density of bulk CrO₂ is used, an equivalent M_s of 20 emu/g can be deduced, which is much smaller than the theoretical value, $M_s = 133$ emu/g,¹⁹ corresponding to an integral moment of $2 \mu_B$ per Cr ion as expected for a half metal. However, considering that the density of the nanoparticle-based film should be considerably lower than the bulk value due to its porosity nature, the value of M_s per unit mass is obviously underestimated. The presence of Cr₂O₃ composition may also reduce the deduced value of M_s . However, the contribution of Cr³⁺ oxidation state composition to the total mass is not dominant as discussed above. On the other hand, surface effects can also lead to a decrease of the magnetization of oxide nanoparticles, with respect to the bulk value, due to several different mechanisms,¹⁷ which might be another possible source of the reduction of the saturation magnetization in our nanoparticle sample.

As shown in Fig. 4, temperature dependence of saturation magnetization was taken while warming the film in 10 kOe. The curve has the characteristic of a ferromagnetic film. However, it seems the magnetization drops much slower with temperature than that expected for a polycrystalline CrO₂ film. Below room temperature, the normalized magnetization $M(T)/M(0)$ is about 10%–20% higher than that reported for the CVD fabricated CrO₂ epitaxial film.²⁰ The magnetization measured for our sample may contain the contribution of the antiferromagnetic (AFM) Cr₂O₃ component below its Neel temperature (~ 307 K). This contribution is enhanced for AFM nanoparticles due to superantiferromagnetism, especially at higher applied field. Around room temperature, the drop of magnetization becomes sharper. A Curie temperature (T_C) of about 400 K, corresponding to the T_C of CrO₂, may be estimated from the extrapolation of the temperature-dependent magnetization curve. On the other hand, the magnetization of the sample reflects ferromagnetic hysteresis loop in a wide temperature range, at least up to 150 K. Such temperature is well above the block temperature for common magnetic nanoparticles, at which magnetization curve should exhibit no hysteresis due to superparamagnetism.

CrO₂ is the only ferromagnetic phase among all the oxides of chromium. We believe the ferromagnetic property of our chromium oxide nanoparticle film comes from the nanoscaled CrO₂ composition. We think the growth condition for CrO₂ based clusters through substoichiometric oxide cluster generation and subsequent flow-controlled reaction,

similar to the steps used in the laser ablation experiments of Bergeron *et al.*,⁹ can be realized in the plasma gas aggregation process. In our cluster source, the blow of argon gas to the target surface makes an oxygen-deficiency condition near the target, inducing the nucleation of substoichiometric chromium oxide clusters. Meanwhile, the buffer gas stream of mixed argon and oxygen generates an oxygen-rich condition in the area some distance away from the target surface, where larger clusters grow through the coagulations between smaller nucleuses and are completely passivated through the reaction in the oxygen-rich gas flow. In this process, ferromagnetic properties are preserved upon cluster growth within the specific Cr_{*n*}O_{2*n*+2} serial.

In summary, a smooth film of densely packing spheric chromium oxide nanoparticles has been successfully fabricated by deposition of chromium oxide clusters generated with a reactive magnetron plasma gas aggregation source under high-vacuum and room temperature. A magnetic hysteresis loop similar to polycrystalline CrO₂ bulk film was observed, with an enhanced coercive field of 168 Oe. The rise in the ferromagnetic property was attributed to the nanoscale CrO₂ composition. Our work demonstrates a simple high-vacuum compatible way to fabricate ferromagnetic films of chromium oxide nanoparticles under low temperature condition.

We thank the financial support from NSFC (Grant Nos.60478012,10674063, 90606002, and 10674056), the Hi-tech Research and Development Program of China under contract NO. 2006AA03Z316, as well as the the Provincial Hi-tech Research Program of Jiangsu in China (BG2007041).

¹K. Schwarz, *J. Phys. F: Met. Phys.* **16**, L211 (1986).

²K. P. Kamper, W. Schmitt, and G. Guntherodt, *Phys. Rev. Lett.* **59**, 2788 (1987).

³A. Gupta, X. W. Li, and G. Xiao, *J. Appl. Phys.* **87**, 6073 (2000).

⁴X. W. Li, A. Gupta, T. R. McGuire, P. R. Duncombe, and G. Xiao, *J. Appl. Phys.* **85**, 5585 (1999).

⁵P. G. Ivanov, S. M. Watts, and D. M. Lind, *J. Appl. Phys.* **89**, 1035 (2001).

⁶A. Anguelouch, A. Gupta, G. Xiao, D. W. Abraham, Y. Ji, S. Ingvarsson, and C. L. Chien, *Phys. Rev. B* **64**, 180408 (2001).

⁷N. Popovici, M. L. Paramês, R. C. da Silva, O. Monnereau, P. M. Sousa, A. J. Silvestre, and O. Conde, *Appl. Phys. A: Mater. Sci. Process.* **79**, 1409 (2004).

⁸K. Wegner, P. Piseri, H. V. Tafreshi, and P. Milani, *J. Phys. D* **39**, R439 (2006).

⁹D. E. Bergeron, A. W. Castleman, Jr., N. O. Jones, and S. N. Khanna, *Nano Lett.* **4**, 261 (2004).

¹⁰H. Haberland, M. Mall, M. Moseler, Y. Qiang, T. Reiners, and Y. Thurner, *J. Vac. Sci. Technol. A* **12**, 2925 (1994).

¹¹R. H. Cheng, B. Xu, C. N. Borca, A. Sokolov, C.-S. Yang, L. Yuan, S.-H. Liou, B. Doudin, and P. A. Dowben, *Appl. Phys. Lett.* **79**, 3122 (2001).

¹²D. Gall, R. Gampp, H. P. Lang, and P. Oelhafen, *J. Vac. Sci. Technol. A* **14**, 374 (1996).

¹³M. N. Iliiev, A. P. Litvinchuk, H. G. Lee, C. W. Chu, A. Barry, and J. M. D. Coey, *Phys. Status Solidi B* **215**, 643 (1999).

¹⁴J. Zuo, C. Y. Xu, B. H. Hou, C. S. Wang, Y. Xie, and Y. T. Qian, *J. Raman Spectrosc.* **27**, 921 (1996).

¹⁵H. Y. Hwang and S.-W. Cheong, *Science* **278**, 1607 (1997).

¹⁶R. K. Zheng, H. Liu, Y. Wang, and X. X. Zhang, *Appl. Phys. Lett.* **84**, 702 (2004).

¹⁷A.-H. Lu, E. L. Salabas, and F. Schüth, *Angew. Chem., Int. Ed.* **46**, 1222 (2007).

¹⁸D. L. Leslie-Pelecky and R. D. Rieke, *Chem. Mater.* **8**, 1770 (1996).

¹⁹J. M. D. Coey and M. Venkatesan, *J. Appl. Phys.* **91**, 8345 (2002).

²⁰X. W. Li, A. Gupta, and G. Xiao, *Appl. Phys. Lett.* **75**, 713 (1999).